The influence of low-level wind shear on the surface turbulence kinetic energy production in Adventdalen, Svalbard

Charalampos Sarchosidis and Milan Klöwer

March 4, 2016

Abstract

Turbulence in the atmospheric boundary layer is an importance process for the dissipation of energy in the global energy cycle. As turbulence acts on time and length scales smaller than resolved by numerical models, its effect on weather and climate is usually insufficiently parametrized. Being usually stably stratified within the lower hundreds of meters the Arctic atmospheric boundary layer provides further enhanced challenge for numerical weather prediction and climate projections. Improving the understanding of factors controlling turbulence kinetic energy (TKE) in Arctic environments potentially advances the prediction of societally important extreme weather events of local climate change. In this study, the TKE budget is presented for two stations in Adventdalen, Svalbard during a field work campaign from Feb 8-15, 2016. The turbulence is primarily in the regime of forced convection, hence shear instability production of turbulence is the main controlling factor. Strong low-level wind shear is used as a necessary but insufficient definition for low-level jets, a common feature of the wintertime Arctic boundary layer. Wind shear within the lower 200m is found to have a large impact on the TKE production at one of the stations. However, the vicinity of a Fjord for the other station dominates over the effect of low-level wind shear. It is concluded that further data is needed to isolate clearly the effect of low-level jets on the TKE budget close to fjords.

1 Introduction

The atmospheric boundary layer (ABL) is the lowermost part of the atmosphere that experiences directly the impact of the planetary surface and adapts accordingly to radiative forcing on time scales of less than an hour. Numerical weather prediction models as well as climate models struggle in representing phenomena in the ABL, due to unresolved turbulence, associated heat and momentum fluxes and complex orography. Parametrizations for those processes are often not sophisticated enough and are therefore one of the main error sources in numerical models. An improved understanding of these surface processes presumably advances weather forecasting as well as climate projections (Banta et al., 2006). Although turbulence close to the surface acts primarily on time and length scales orders of magnitude smaller than weather and climate it is still societally relevant due to its ability to transfer signals across scales. Therefore, a better representation of processes classically defined as micrometeorology would also project on the larger societally important meteorological variables, such as extreme weather events or regional climate change.

One of the most important variables in micrometeorology is the turbulence kinetic energy (TKE), a measure of the intensity of turbulence. The TKE is directly related to the transport of momentum, heat and moisture through the ABL (Stull, 1988). It is usually

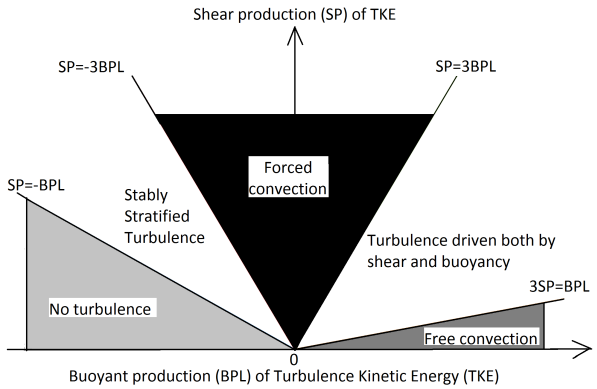

Figure 1: **Relation between the mechanical and the buoyant term.** Forced convection is the result dominating mechanical term compared to the buoyant term. Free convection occurs when the buoyant term is large and positive, whereas the flow is laminar for large and negative buoyant term. Adapted from Stull, 1988.

expressed per unit mass m

$$\overline{e} = \frac{1}{2}\overline{(u'^2 + v'^2 + w'^2)} \tag{1}$$

where u, v, w are the wind components, and the prime denotes the deviation from the Reynolds average (see Appendix A.1). Regarding energy transformations and reservoirs on a global scale, as estimated by the Lorenz energy cycle (Holton, 2004), clarifies the importance of TKE as part of this cycle. Dissipation of kinetic energy arises through turbulence in the atmospheric boundary layer, which is the main process allowing energy to leave the cycle.

Turbulence in the ABL can be generated thermally and mechanically. Thermal turbulence (i.e. free convection) is generated due to diabatic heating, which, if strong enough, favours air, that is hence warmer than its environment, to rise. Thermal production of turbulence therefore arises from buoyancy forces (Wallace and Hobbs, 2006). Thermal turbulence is usually small in polar regions,

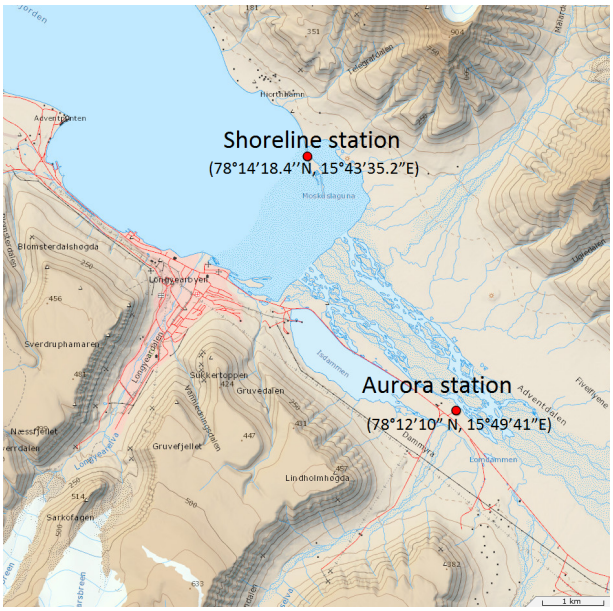

Figure 2: **Map of the area around Longyearbyen.** A sonic anemometer is installed at both the Shoreline station as well as at the Aurora station. A SODAR is installed at the Aurora station. The coordinates are given in the Figure.

especially away from the sea, since open sea water is the only heating source during winter. Mechanical production of turbulence (i.e. forced convection), however, arises from shear instability due to frictional drag close to the surface. Mechanical turbulence can not be assumed to be small in presence of winds, and is largely amplified for rough surfaces and complex orography, which is given in regions like Svalbard.

We derive the production of TKE from the Navier-Stokes-equations. Transforming the momentum equation into an equation for the kinetic energy and applying Reynolds decomposition (Appendix A.1) yields a prognostic equation for the turbulence kinetic energy $\overline{e}$ (hereafter referred to as *turbulence kinetic energy budget*). Assuming horizontal homogeinity, neglecting subsidence and choosing a coordinate system that is aligned with the mean wind (Appendix A.2) simpli-

fies the equation to

$$\frac{\partial \overline{e}}{\partial t} = \frac{g}{\overline{\theta_v}}(\overline{w'\theta'_v}) - (\overline{u'w'})\frac{\partial \overline{u}}{\partial z} - \frac{\partial(\overline{w'e})}{\partial z} - \frac{1}{\overline{\rho}}\frac{\partial(\overline{w'p'})}{\partial z} - \epsilon \quad (2)$$

where $\frac{\partial \overline{e}}{\partial t}$ is the turbulence kinetic energy tendency, g the gravitational accelaration, $\theta_v = \overline{\theta_v} + \theta'_v$ the Reynolds decomposed virtual temperature, p the pressure, $\overline{\rho}$ the mean density, z the vertical coordinate and ϵ the dissipation rate.

The first term on the right-hand side increases turbulence if $\overline{w'\theta'_v} > 0$, i.e. the vertical velocity anomaly and the temperature anomaly covary (usually for unstable stratification). However, this term reduces the turbulence in the case that $\overline{w'\theta'_v} < 0$ (usually for a stable stratification). As this is physically determined by buoyant forces, this term is referred to as *buoyancy term*. The second term on the right-hand side is a production term only, that increases the turbulence due to wind shear by the process of shear instability. The third term on the right-hand side is referred to as convergence of TKE, but usually small and therefore ignored (Stull, 1988). Same holds for the forth term, which arises from the convergence of pressure perturbations. The last term represents the viscous dissipation of the turbulent kinetic energy. As hard to calculate with the available measurements, dissipation is not taken into account in the present study. Closing the TKE budget is a challenge, with issues arising from the lack of data and their accuracy.

The ratio between the buoyancy and the mechanical term, is the flux Richardson number

$$R_f = \frac{\text{buoyancy term}}{\text{mechanical term}} = \frac{\frac{g}{\overline{\theta_v}}\overline{w'\theta'_v}}{-\overline{u'w'}\frac{\partial \overline{u}}{\partial z}} \quad (3)$$

describing the relative importance of the two main production terms. $R_f = -1$ can be regarded as a critical value for distinguishing between stable and unstable flows. For $R_f > -1$ the flow *is* turbulent, whereas for $R_f < -1$ the flow *becomes* laminar (Stull, 1988). This can also be seen in Figure 1 depicting the contributions of the buoyancy and shear terms to the nature of turbulence. The regime with no turbulence is seen for $R_f < -1$. Turbulence is mainly mechanical (forced convection) for $-\frac{1}{3} < R_f < \frac{1}{3}$ when the buoyancy is comparably small. Turbulence is considered to be mainly thermal for $R_f > 3$, which corresponds to the case of free convection.

The turbulence generation is especially interesting in polar regions during wintertime due to the seasonal absence of sunlight, which stabilizes the air column via surface cooling. Therefore suppression of mixing can occur, which allows smaller-scale features, like weak, sporadic turbulence near the surface, to persist, thus complicating the flow (Banta, 2006). The polar ABL can be as thin as hundred meters, whereas in the tropics, strong convection causes its thickness up to a few kilometers (Stull, 1988). In general, the ABL thickness varies considerably in space and time.

An important and common feature in the ABL is the low-level jet (LLJ), that generates turbulence generation through the mechanical term. It is described as a thin stream of fast moving air, with maximum wind speeds of 10 to 20 ms^{-1} usually located 100 to 300 m above the ground even though the ABL might be stable and the winds calm near the surface. Within a low-level jet wind speeds can reach 30 ms^{-1} and its vertical extent might be as high as 900 m. The LLJ can have a width of hundreds of kilometres and usually forms during night peaking during the predawn hours. Stull, 1988 suggests the LLJ to be defined as a relative wind speed maximum that is more than 2 ms^{-1} faster than aloft and below within the lowest 1500 m of

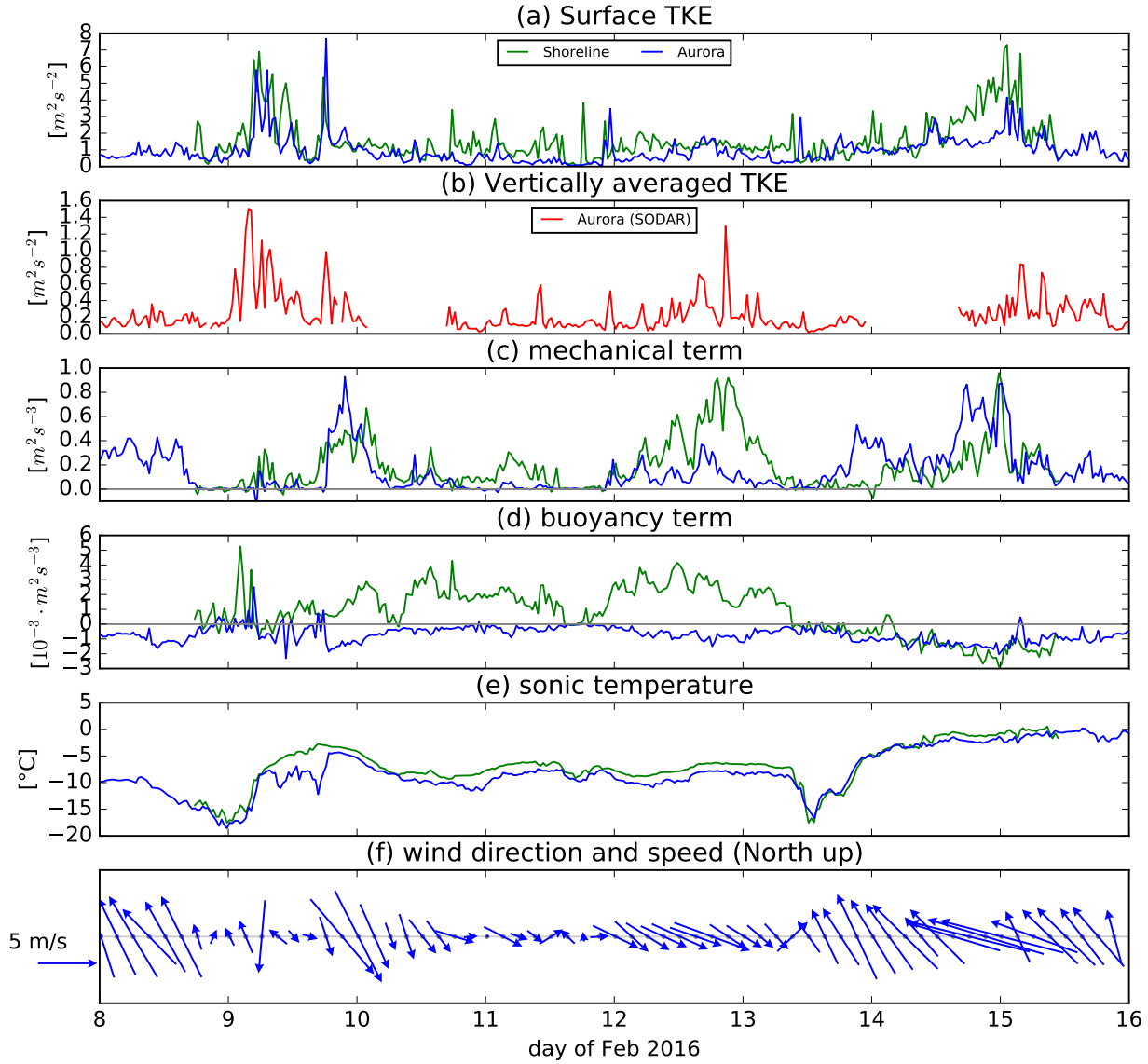

Figure 3: **Temporal evolution of main quantities during the fieldwork campaign in Adventdalen, Svalbard at Shoreline and Aurora station**. (a) Turbulence kinetic energy (TKE); (b) vertically averaged TKE from SODAR data; (c) mechanical term; (d) buoyancy term; (e) sonic temperature; (f) mean wind speed and direction. Averaging period is $\tau = 30$min.

the atmosphere.

The LLJ is responsible for generating wind shear in the ABL and is thus a source of turbulent fluxes, that can potentially propagate downward to the surface. In the absence of a LLJ, the turbulence is rather generated at the surface and transported upward.

In the present study, we calculate the TKE, the mechanical term and the buoyancy term from sonic anemometer measurements at two stations in Adventdalen, Svalbard for Feb 8 - Feb 15, 2016, the period of the field work campaign. Possible low-level jets are identified from vertical wind profiles at one of the stations. However, due to the quality of data, we note, that our defintion for identifying low-level jets may also include strong wind events, without the typical jet structure. We therefore restrict our conclusion to the influence of low-level wind shear events on the surface TKE. Their influence on the surface kinetic energy terms is analysed by statistical means. Section 2 describes the instruments used and the processing of the data (section 2.2). The results are presented in section 3 with a brief introduction to the weather situation during the field work campaign (section 3.1). Finally, section 4 draws a conclusion and includes some discussion and an outlook. The appendix A provides some details about the methodology.

2 Data and methodology

2.1 Data

During the field work campaign a Campbell weather station was set up 2.5 km North-East of Longyearbyen (the Shoreline station, 78°14'18.4"N, 15°43'35.2"E) with a 4m distance from the sea and 1m above sea level. The station consisted of 2 mechanical anemometers at 1 and 3m height relative to the ground measuring at 1 Hz temporal resolution. At a height of 2m a CSAT 3D sonic anemometer measured wind velocity at a frequency of 20 Hz (Further details concerning accracy are described in Gilson and Samuelsen, 2016). It was set up in the afternoon of Feb 8, 2016 and started logging at 17h (local time) until Feb 15, 2016 11h. The sonic anemometer during that period is almost complete, except for a few minutes missing during the period. However, the mechanical anemometers provide only incomplete data, hence, they were not used for this study.

The Aurora station, 4.5 km ESE of Longyearbyen (78°12'10"N, 15°49'41"E), is the second station equipped with a sonic anemometer, that is continuously measuring. In the present study, data from Feb 8, 0h to Feb 16, 0h is used to cover approximately the same time span. At a height of 1m and 10m there are two mechanical anemometers, measuring at 1 Hz temporal resolution. Although their data is fully available, for consistency with the Shoreline station the use of this data is neglected.

Furthermore, a SODAR (i.e. SODAR-RASS, Sonic Detection and Ranging, Radio Acoustic Sounding System) is located at the Aurora station, a Scintec MFAS versatile acoustic profiler measuring wind and turbulence up to 1000 m above the ground (Scintec AG, Rottenburg, Germany). The operation is based on the reflection of acoustic pulses at temperature inhomogeneities in the air with subsequent doppler analysis. Measurement frequency is 1/10min. Minimum height level for the measurements is 30 m, but the maximum height depends on the atmospheric conditions. During calm days, for example, measurements can reach up to 800 m, but during windy days they may not even surpass 300 m. SODAR data is used from Feb 8, 0h to Feb 16, 0h. The vertical resolution is 10m and the accuracy of the horizontal wind speed is 0.1 to 0.3 ms^{-1}.

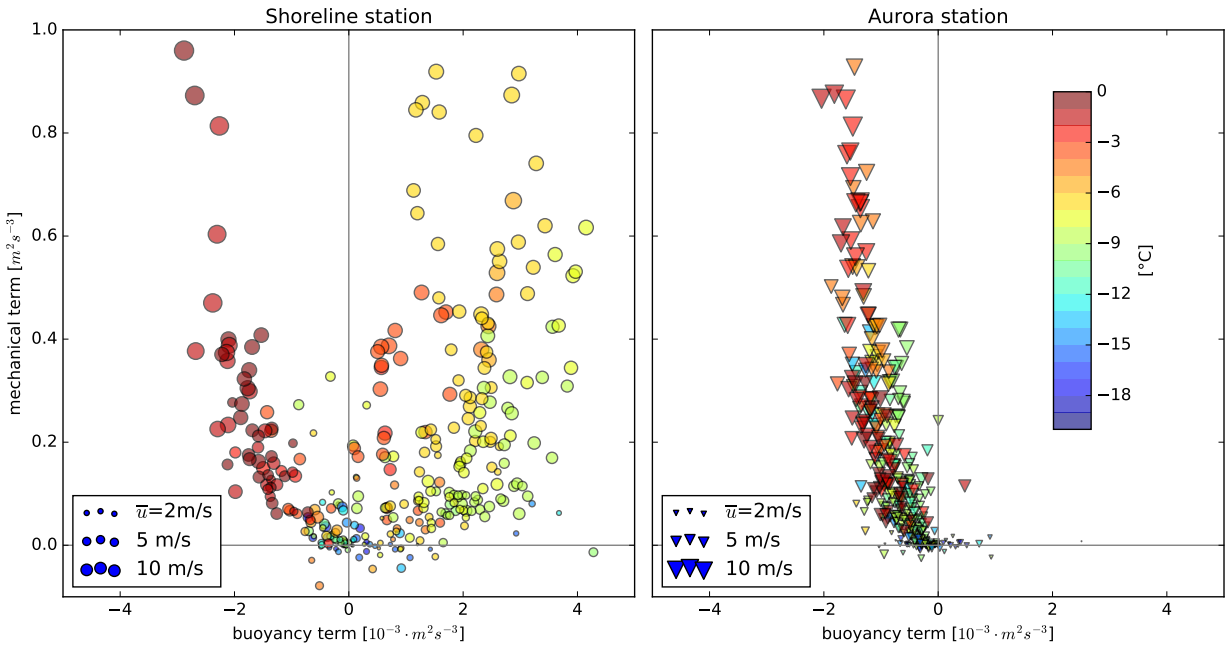

Figure 4: **Surface turbulence is dominated by shear instability.** Relation between buoyancy term, mechanical term, sonic temperature θ_s (color-shaded), and mean wind speed ($\overline{u}$ after rotation, marker size) for both the Shoreline station (a) and the Aurora station (b) from Feb 8 to Feb 15, 2016. Grey shaded areas correspond to forced convection with flux Richardson number $|R_f| < \frac{1}{3}$, as adapted from Stull, 1988. Please note, that the y-axis is rescaled for readability as given in the label.

2.2 Methodology

The calculation of the surface energy budget terms is done by means of Reynolds decomposition (see appendix A.1) with an averaging period of $\tau = 30$min. The averaging periods are the same for all data, always spanning from on the hour to 30min past and from 30min past to on the next hour. For each period, the wind vectors were rotated to correct for yaw and pitch (see appendix A.2) and in order to simplify equation 2. The sonic temperature θ_s is assumed to be equal to the virtual temperature θ_v, as their difference is negligible and a correction would require unavailable information about humidity and pressure.

The wind shear term $\frac{\partial \overline{u}}{\partial z}$ is estimated from $\frac{\overline{u}-0}{2\ \mathrm{m}}$, hence assuming a linear wind decrease from the sonic anemometer height of 2m to a wind speed of 0 at the ground. Although a better estimation would be possible from the mechanical wind anemometers at both stations, this was not done for a consistent comparison between the two stations, as this data is missing for most of the time at the Shoreline station. Calculating the mean vertical shear of the horizontal wind from mechanical anemometers at the Aurora station suggests that the mechanical term might be overestimated by a factor of 2 or so.

3 Results

3.1 Weather situation

On a synoptic scale, the weather in Adventdalen was dominated by south-easterlies (i.e. down-valley winds) on February 8, 2016, but it changed to weaker north-westerlies (i.e. up-valley winds) on the following day, that lasted until Feb 13, afternoon (Fig. 3f). During the last two days of the field work campaign Advantdalen experienced stronger winds from South-East. The synoptic signal can also be seen in the 2m-temperature measured by the sonic anemometer: Wind-reversals are usually associated with weaker winds, espacially during the night from Feb 8 to Feb 9 around 0h00 and Feb 13, afternoon, and are presumably related to drops in surface temperature up to 10°C (Fig. 3e). Further analysis on the weather situation during the field work week can be found in Valkonen and Kapari, 2016.

These synoptic scale influences, are assumed to have a considerable effect on the surface energy balance, especially since north-westerlies blow from Adventfjorden and Isfjorden into the valley, and south-westerlies vice versa. However, this is not the main focus of this study and is addressed in more detail elsewhere (Gilson and Samuelsen, 2016)

3.2 Surface turbulence kinetic energy budget

The surface TKE at both Shoreline and Aurora station are of comparable magnitude and variability (Fig. 3a). Compared to the vertically averaged TKE as obtained from the SODAR (Fig. 3b), we find signals, that occur simultaneously at both stations and in the lower hundreds of meters in the atmosphere, which points towards situations where the TKE is forced by large scale weather influences. However, some events of high TKE are only observed in the vertical but not at the surface (e.g. Feb 12, 23h), which indicates a decoupling of the surface with the atmosphere above.

The two main production terms for TKE, the mechanical term (Fig. 3c) and the buoyancy term (Fig. 3d), are analysed for the events in high TKE values: Some of the high TKE events are apparently connected to mechanical production of turbulence (Feb 9, 21h to Feb 10, 3h and Feb 14, 18h to Feb 15, 3h), whereas some periods with a large me-

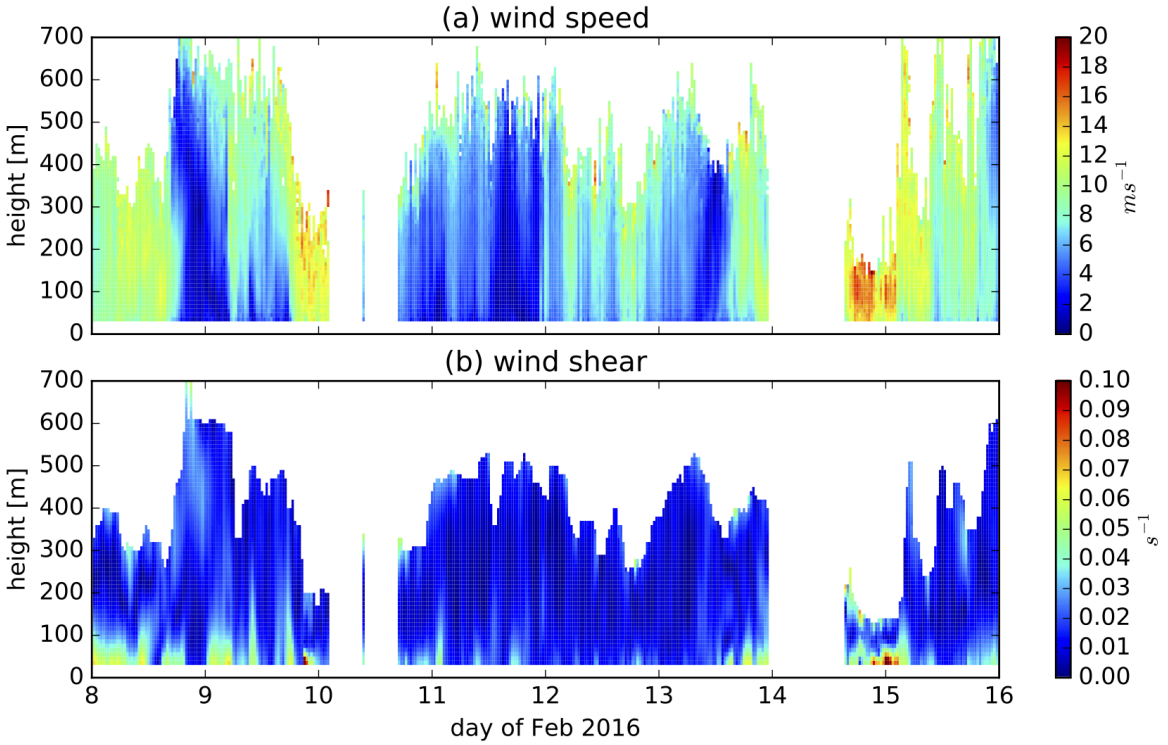

Figure 5: **Vertical profiles of the horizontal wind speed $\overline{u}$ (a) and vertical shear of the horizontal wind $|\frac{\partial \overline{u}}{\partial z}|$ (b)** measured by the SODAR at the Aurora station from Feb 8 to Feb 15, 2016. White areas indicate no data. The wind is rotated so that $\overline{v} = \overline{w} = 0$ (see Appendix A.2)

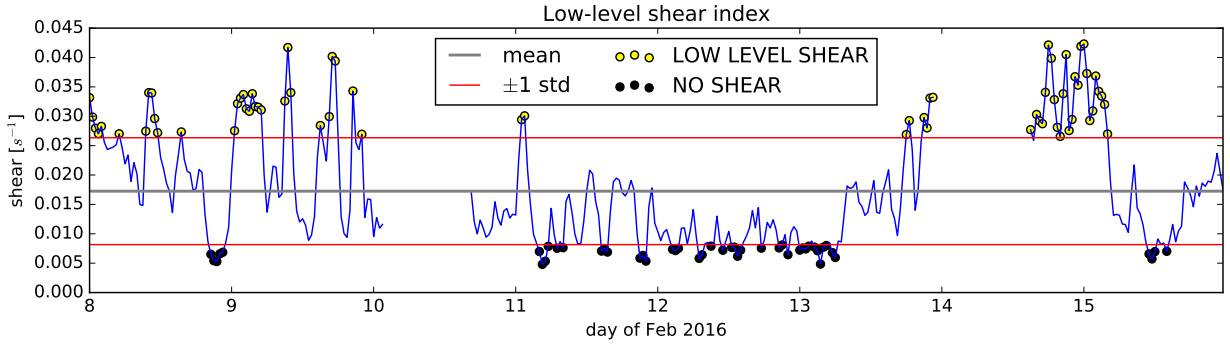

Figure 6: **Index for low-level wind shear events.** Vertical mean of horizontal wind shear between 40 and 200m from SODAR data. The grey line indicates the mean and the red lines a one standard deviation threshold for identifying a presence of strong low-level shear (above +1 std, called LOW LEVEL SHEAR, hereafter) or of no jet (below -1 std, called NO SHEAR, hereafter). This definition includes low-level jets, but we note that strong winds without satisfying the typical low-level jet criteria are presumably not excluded from this index.

chanical term, seem to not be reflected in the surface TKE (Feb 12, 18h - Feb 13, 2h).

When it comes to the buoyancy term (Figure 3d), we see an interesting, yet reasonable, difference between the two stations. The buoyancy is mostly negative at the Aurora station, which we interpret by the ground being totally covered by snow and ice, hence providing diabatic cooling from below. There is no heating source around the station in contrast to the Shoreline station, where the open sea makes the air potentially positively buoyant. But despite the positive values here, the buoyancy term is still O(10^{-3}) smaller than the mechanical term, which is to be expected in polar regions during wintertime.

In analogy to Figure 1, we relate the mechanical and buoyancy term for the Shoreline and the Aurora station seperately in order to investigate their dependence on mean wind speed and 2m temperature (Fig. 4). Analysing the flux Richardson number R_f leads to the conclusion that the turbulence is largely dominated by forced convection, i.e. cases where the mechanical production is orders of magnitude larger than the buoyancy term. These findings are supported by the absence of diabatic heating (except for some heating from open water at the Fjord close to the Shoreline station) during the field work campaign, which took place during polar night.

There is a general tendency of the mechanical term to be larger for stronger wind speeds at 2m (Fig. 4), which can be understood via the increase of vertical wind shear close to the surface. The Aurora station shows largest values in the mechanical term also for temperatures above -6°C, which we relate to the synoptic situation, as strong winds were associated with warmer temperatures during the field work campaign (Fig 3e and f). The buoyancy term at the Shoreline station has both negative and positive values. However, the positive values seem to be connected to colder temperatures (-12°C to -6°C) in contrast to the negative values that occured during periods of warmer temperatures (above -3°). We conclude that the strength of the synoptic scale advection of heat influences the surface stratification (as the surface is still comparably cold) and therefore permitting or prohibiting weak thermal convection, which is reflected in the sign of the buoyancy term.

3.3 Influence of low-level wind shear

In order to identify occurences of low-level jets, vertical profiles of wind speed and vertical wind shear are analysed from SODAR data (Fig. 5). Missing data usually occurs above a certain height in the case of strong wind speed below, that decreases the data quality above (e.g. Feb 15 around 0h) the classical definition of a low-level jet, i.e. wind speed maximum $> 2\text{ms}^{-1}$ higher than aloft and below within the lowest 1500m of the atmosphere, is therefore hardly applicable. Based on the data quality, we choose a definition that relies on the mean vertical wind shear within the lower 200m of the atmosphere. This yields a low-level shear index (Fig. 6), which is used to distinguish between events of high low-level shear (called LOW LEVEL SHEAR hereafter) and weak low-level shear (called NO SHEAR hereafter). They are defined by a one standard deviation difference with respect to the mean of the low-level shear index. Regarding the vertical profiles of wind speed for LOW LEVEL SHEAR (Fig. 7) indicates that this definition includes low-level jets but also cases with solely strong shear within the lower 200m and do not satisfy the above mentioned classical defintion of a low-level jet. However, the mean profiles satisfy the classical definition, but might be biased due to differences in the

maximum height of SODAR data. Nevertheless, we proceed with this definition, keeping in mind that the index designed to identify low-level jets is contaminated with strong wind events.

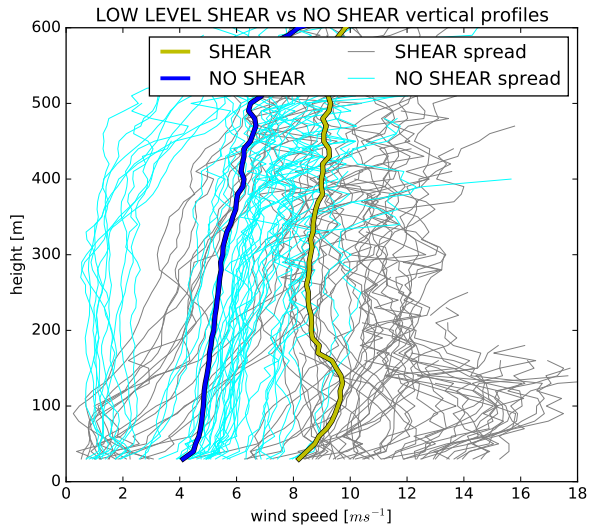

Figure 7: **Vertical mean wind speed profiles for LOW LEVEL SHEAR versus NO SHEAR**. Using the definition from Fig. 6, individuals profiles are identified from Fig. 5 and given in thin lines. Thick lines represent the LOW LEVEL SHEAR, NO SHEAR mean respectively.

To investigate the influence of low-level jets, i.e. in terms of our LOW LEVEL SHEAR, NO SHEAR definition, on the surface TKE budget, we make use of the analysis behind Fig. 4. Conditionally mask the measurements that are not within LOW LEVEL SHEAR, NO SHEAR reveals the properties of the surface TKE budget for these events (Fig. 8). Strong low-level wind shear affect the TKE budget at the Aurora station by increasing the mechanical term (Fig. 8b and d). Therefore we conclude that the ABL at the Aurora station experiences downward transport of TKE for the case of strong wind shear in the lower 200m. In contrast, strong low-level wind shear occuring at the Shoreline station affects the sign of the buoyancy term. LOW LEVEL SHEAR is associated with negative buoyancy terms, whereas NO SHEAR is associated with positive buoyancy terms. The conclusion is that low-level wind shear affects the mechanical term at the Aurora station, whereas it affects the buoyancy term at the Shoreline station. At the Aurora station, this corresponds to the theory of having turbulence propagating downward from the ABL to the surface. However, at the Shoreline station we might observe solely the influence of the wind direction and therefore associated heat fluxes from the Fjord. This can be understood in a way, that all LOW LEVEL SHEAR events are associated with south-easterly winds, hence a down-valley wind, that presumably reduces the influence of the Fjord, as air is advected from the valley rather than from the Fjord (Fig. 3f). In turn, NO SHEAR events are mainly occurring during phase of north-westerly winds, coming therefore from the Fjord. These events presumably result in advection of heat fluxes from the open water and hence, affecting the stratification close the surface in the vicinity of the Shoreline station. We summarize therefore, that the Shoreline station feels strongly the influence of the Fjord, whereas this influence is weak at the Aurora station.

4 Concluding discussions

This study presents the turbulence kinetic energy budget close to the surface at two stations in Adventdalen, Svalbard measured by means of sonic anemometers during a field work campaign from Feb 8 to Feb 15, 2016. Although it is impossible to close the budget from available data, the relative importance provides insight to the factors controlling the budget during different weather situations, with a special focus on the occurences of strong low-level wind shear, which can be re-

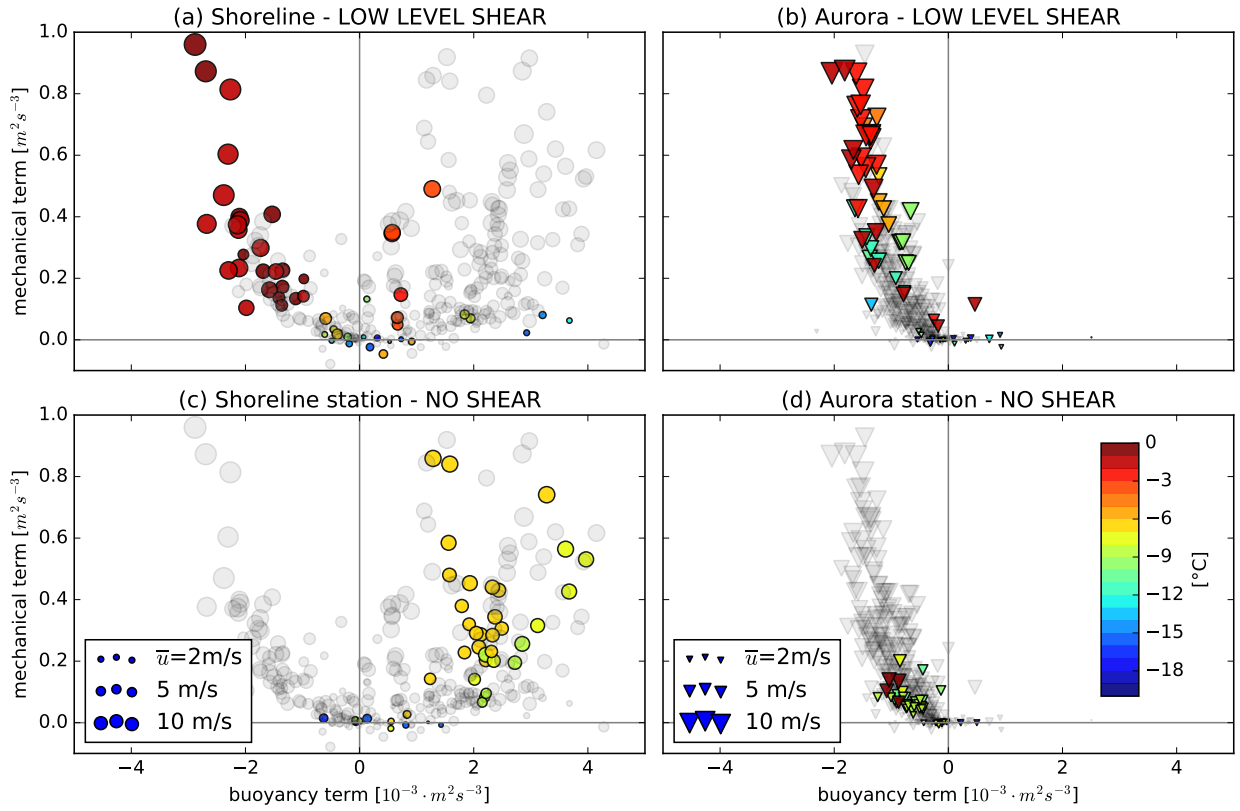

Figure 8: **Influence of low-level wind shear on the surface turbulence kinetic energy budget.** Statistical relation between buoyancy term, shear production, sonic temperature T_s (color-shaded), and mean wind speed at 2m height ($\overline{u}$ after rotation, marker size) for both the Shoreline station (a,c) and the Aurora station (b,d) under the condition of LOW LEVEL SHEAR (a,b) or NO SHEAR (c,d) from Feb 8 to Feb 15, 2016. Grey markers correspond to the measurements where the condition is not fulfilled. Grey shaded areas correspond to forced convection (with flux Richardson number $|R_f| < \frac{1}{3}$, as adapted from Stull, 1988).

garded as a necessary but not sufficient condition to identify low-level jets. The vertical shear of the horizontal wind is identified by means of a SODAR, that is located at one of the stations.

The synoptic weather situation during the field work campaign consists basically of two regimes: Winds coming from the South-East correspond to down-valley winds towards Adventfjorden and Isfjorden, whereas winds coming from the North-West are blowing up-valley from the fjords into Adventdalen. The weather situation is important to understand the underlying physical connections for all statistical relations that are drawn in this study.

Investigating the relative importance of the mechanical term and the buoyancy term in producing turbulence kinetic energy leads to the conclusion that turbulence is primarily in the regime of forced convection, with the mechanical terms being several orders of magnitude larger than the buoyancy term. This is put into relation with the local climate in Svalbard during polar night, where the absence of sunlight disables largely convection to arise from surface heating. An exception occurs close to open water, as relatively warm sea surface temperatures provide a source for surface heat fluxes, which influence is still weak on the turbulence kinetic energy compared to the mechanical term.

This exception is observed at the Shoreline station, where the buoyancy term is both positive and negative, depending on the prevailing wind direction and the advection of heat associated with it. This is not the case at the Aurora station, where the buoyancy term is almost always negative, presumably due to the vicinity being entirely covered with snow and ice, which has a stabilizing affect on the stratification close to the surface.

Low-level wind shear is observed to increase strongly the mechanical term in the turbulence kinetic energy budget at the surface in the vicinity of the Aurora station, which fits to the theory of having turbulence that is produced in layers of strong shear then propagates down from the ABL towards the surface. Comparing the low-level wind shear influence on the turbulence kinetic energy budget close to the Shoreline station reveals another reasoning: The majority of the events with strong (weak) low-level wind shear occur during phases with winds blowing from South-East (North-West), hence minimizing (enhancing) the effect of the Fjord on the Shoreline station due to advection of air masses from Adventdalen (Adventfjorden and Isfjorden).

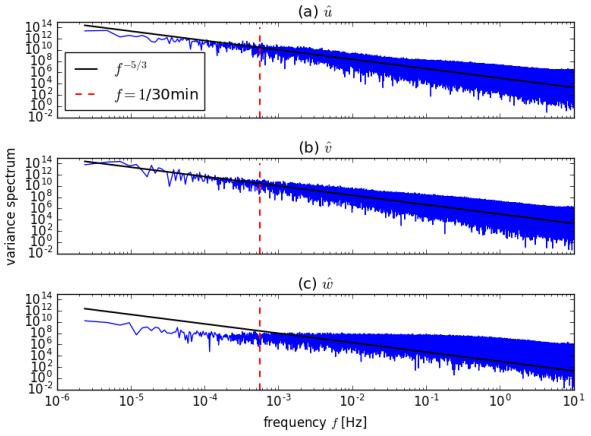

Figure 9: **Variance spectra for wind components** u, v, w measured with a sonic anemometer at the Aurora station in Adventalen, Svalbard. The winds are not rotated and therefore may include some yaw and pitch of the measurement device. Black lines illustrate the power law for a turbulent fluid from Kolmogorov's -5/3 theory. Red vertical lines correspond to the averaging time scale $\tau = 30\text{min}$. Measurement height is 2m above ground.

In order to increase the strength of scientific conclusion about the low-level jet influence on the turbulence kinetic energy we therefore point to the necessity of vertical

wind profiles with a larger vertical extent. This would allow a more robust identification of low-level jets. Furthermore, an extended field work campaign, with a larger spread in the weather situations would be necessary to draw more weather-independent conclusions on the influence of low-level jets. Although low-level jets only occur in certain weather situations, a larger spread in those would set a more robust scientific conclusion into perspective.

A Appendix

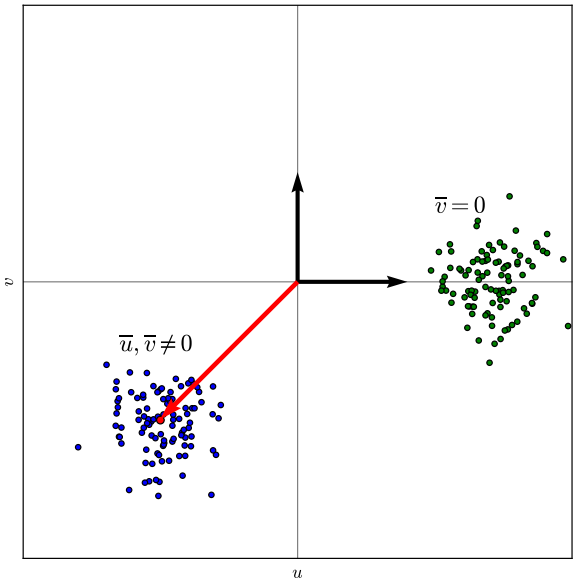

Figure 10: **Yaw and pitch correction for wind measurements from sonic anemometer.** For each averaging period the wind components u, v, w are rotated (blue circles before rotation, green circles after) so that the u-axis is aligned with the mean wind $((\overline{u}, \overline{v})$, red arrow). This procedure is repeated in the u, w plane. This satisfies $\overline{v} = \overline{w} = 0$ and therefore simplifies the surface turbulence kinetic energy balance equation.

A.1 Reynolds decomposition

The derivation of the surface turbulence kinetic energy budget relies on a Reynolds decomposition of the underlying energy equation. This decomposition states that a variable $\phi = \phi(t)$, where t refers to either a spatial or the temporal dimension (here t is time), can be split into a mean (denoted with an overbar) and an anomaly (denoted with a prime) by

$$\phi = \overline{\phi} + \phi' \tag{4}$$

where $\overline{\phi}$ is considered to be constant over the averaging time period τ. In the case where ϕ fluctuates on clearly seperable time scales, so that ϕ' is actually stationary during the period τ, the Reynolds decomposition is applicable. In a spectral sense, this means, the averaging time scale τ is supposed to be chosen within a spectral gap of ϕ. In the case of no spectral gap (i.e. all frequencies of ϕ show some non-negligible variance) there is in general no constant $\overline{\phi}$ and therefore ϕ' can not be considered as stationary. For the measurements of u, v, w from the sonic anemometer at the Aurora station the variance spectrum is shown in Fig. 9 (the one at the Shoreline station yields virtually the same results). The spectrum of the horizontal wind is observed to be in close agreement with Kolmogorov's -5/3 law, which states the spectral energy distribution within a fully turbulent fluid. Based on this, there is some evidence for the boundary layer in Adventdalen to be turbulent on time scales from milliseconds to weeks. However, the spectrum might not be stationary, so that the one shown in Fig. 9 might actually be a superposition of different spectra apparent during different local weather regimes. Based on the results from Foken, 2008 we choose an averaging period of $\tau = 30$min, although we note, that one problem of the surface turbulence kinetic energy closure could arise, as the Reynolds decom-

position is not applicable.

A.2 Wind rotation

The wind measurements $u(t), v(t), w(t)$ are rotated for each averaging period of length τ, in order to simplify the surface turbulence kinetic energy budget (equation 2), as the orientation of the coordinate system is arbitrary. For the case, where the mean wind $(\overline{u}, \overline{v}, \overline{w})$ is aligned with the u-axis of the coordinate system, so that $\overline{v} = \overline{w} = 0$, several terms in equation 2 vanish. The rotation is done as follows: Let $\mathbf{u} = (u, v, w)$ be the unrotated wind, $\mathbf{u}_y = (u_y, v_y, w)$ be the wind after horizontal rotation (i.e. yaw correction), and $\mathbf{u}_r = (u_r, v_y, w_r)$ be the wind after both horizontal and vertical rotation (i.e. yaw and pitch correction). Then

$$\mathbf{u}_y = \mathbf{Y}\mathbf{u} \tag{5a}$$

$$\mathbf{u}_r = \mathbf{P}\mathbf{u}_y \tag{5b}$$

with

$$\mathbf{Y} = \begin{pmatrix} \frac{\overline{u}}{\sqrt{\overline{u}^2+\overline{v}^2}} & \frac{\overline{v}}{\sqrt{\overline{u}^2+\overline{v}^2}} & 0 \\ \frac{-\overline{v}}{\sqrt{\overline{u}^2+\overline{v}^2}} & \frac{\overline{u}}{\sqrt{\overline{u}^2+\overline{v}^2}} & 0 \\ 0 & 0 & 1 \end{pmatrix} \tag{5c}$$

$$\mathbf{P} = \begin{pmatrix} \frac{\overline{u}_y}{\sqrt{\overline{u}_y^2+\overline{w}^2}} & 0 & \frac{\overline{w}}{\sqrt{\overline{u}_y^2+\overline{w}^2}} \\ 0 & 1 & 0 \\ \frac{-\overline{w}}{\sqrt{\overline{u}_y^2+\overline{w}^2}} & 0 & \frac{\overline{u}_y}{\sqrt{\overline{u}_y^2+\overline{w}^2}} \end{pmatrix} \tag{5d}$$

where $\mathbf{Y}, \mathbf{P}$ are the rotation matrices to account for yaw and pitch, respectively. This procedure is illustrated in Fig. 10.

References

Banta, R. M., Pichugina, Y. L., & Brewer, W. A. (2006). *Turbulent velocity-variance profiles in the stable boundary layer generated by a nocturnal low-level jet.* Journal of the atmospheric sciences, 63(11), 2700-2719.

Busch, D. M. N., Ebel, D. M. U., Kraus, H., & Schaller, E. (1982). The structure of the subpolar inversion-capped ABL. *Archives for meteorology, geophysics, and bioclimatology, Series A, 31*(1-2), 1-18.

Foken, T. (2008), *The energy balance closure problem: An overview*, Ecological Applications, 18(6), pp. 1351-1367.

Gilson, G. F. and Samuelsen, E. M., 2016. *Mesoscale influence on the surface energy balance at a shoreline station on Svalbard*, Report task 8, AGF-350/850, University Centre in Svalbard.

Holton, J. R. (2004), *An Introduction to Dynamical Meteorlogy*, Elsevier.

Stull, R. (1988), *An Introduction to Boundary Layer Meteorology*, Springer.

Valkonen and Kapari, 2016. *Large scale weather situation.* Report task 4, AGF-350/850, University Centre in Svalbard.

Viana, S., C. Yagüe and G. Maqueda (2009), *Propagation and Effects of a Mesoscale Gravity Wave Over a Weakly-Stratified Nocturnal Boundary Layer During the SABLES2006 Field Campaign*, Boundary-Layer Meteorol., 133:165-188

Wallace, J. M., & Hobbs, P. V. (2006), *Atmospheric science: an introductory survey (Vol. 92).* Academic press.